

# CHARACTERIZATION STUDY OF THE 19<sup>th</sup>-CENTURY INDO-SARACENIC-BULBOUS DOME AT THE MADRAS HIGH COURT, TAMILNADU

## ŠTUDIJA ZNAČILNOSTI INDO-SARACENSKE-ČEBULASTE KUPOLE IZ 19. STOLETJA NA VIŠJEM SODIŠČU V MADRASU, TAMIL NADU, INDIJA

Ravi Ramadoss<sup>1</sup>, Shivakumar Mani<sup>2</sup>, Viswanathan T.S<sup>3</sup>, Ruben Paul Borg<sup>4</sup>,  
S. Thirumalini<sup>5</sup> \*

<sup>1</sup>Dept of civil engineering, SRM Institute of Science & Technology, Kattankulathur, Tamilnadu 603203, India

<sup>2</sup>CoGreen, Ljubljana 1000, Slovenia

<sup>3</sup>School of Civil engineering, VIT University, Vellore, Tamil Nadu, India

<sup>4</sup>Faculty for the Built Environment, University of Malta, Malta

<sup>5</sup>CO<sub>2</sub> Research & Green Technologies, VIT University, Vellore, Tamil Nadu, India

*Prejem rokopisa – received: 2025-02-24; sprejem za objavo – accepted for publication: 2025-12-23*

doi:10.17222/mit.2025.1408

The mortars of the Indo-Saracenic-styled Madras High Court Domes, constructed in 1888–1892 in Madras, Tamil Nadu, were analyzed to investigate their composition, durability, and production technologies. Multiple analytical techniques were employed, including XRD, FT-IR, X-ray Fluorescence (XRF), Thermo-Gravimetric Analysis (TG-DTA), and Scanning Electron Microscopy with Energy-Dispersive X-ray Spectroscopy (SEM-EDX), supported by acid loss and color indexing tests. The binder-to-aggregate ratios of bed-raw mortar (1:2.99), bedding mortar (1:2.94), and external plaster (1:2.74) through acid-digestion analysis. XRD confirmed the dominant calcite peaks (d-spacing  $\approx 0.303$  nm) with secondary silicate and aluminate phases, while FT-IR spectra exhibited carbonate absorption bands at  $\approx 1420$  cm<sup>-1</sup> and  $\approx 875$  cm<sup>-1</sup>, along with organic signatures corresponding to polysaccharides and amide groups. TG-DTA revealed a major weight loss of 40–45% between 600–780 °C, consistent with CaCO<sub>3</sub> decomposition. SEM images showed crystalline hydrated phases of C–S–H and portlandite, whereas EDX analysis indicated oxygen-rich matrices with Ca contents ranging from 18–25 w% and Si contents of 10–12 w%. Acid-loss tests recorded dissolution rates of 7–9%, highlighting the binder's durability. Color indices quantified three distinct pigment layers: hematite-rich red, lead-based yellow, and carbonaceous black. Together, these results demonstrate the use of homogenous mixes and advanced lime-based technologies with organic additives, underscoring the material sophistication of 19<sup>th</sup>-Century construction practices. This comprehensive, quantitatively supported investigation provides critical insights into historic mortar technologies and serves as a scientific basis for conservation strategies of Indo-Saracenic heritage monuments.

Keywords: 19<sup>th</sup> Century Heritage, Masonry domes, lime mortars, chemical analysis, characterization methods

Avtorji članka so analizirali malte kupol višjega sodišča, ki so bile zgrajene v indo-saracenskem slogu med letoma 1888 in 1892 v mestu Madras (sedaj Čenai) v JV indijski državi Tamil Nadu. Zanimala jih je sestava uporabljenih malt, njihova trajnost in tehnologija njihove izdelave. Za analize so avtorji uporabili več analitskih tehnik, vključno z rentgensko difrakcijo (XRD), Fourierjevo Transformacijsko Infrardečo spektroskopijo (FT-IR), rentgensko fluorescenco (XRF), termogravimetrijo z diferencialno termično analizo (TG-DTA) in vrstično elektronsko mikroskopijo z energijsko disperzivno rentgensko spektroskopijo (SEM-EDX), podprto s testi izgube kisline in barvnega indeksiranja. Z analizo kislinke razgradnje so ugotovili razmerja veziva in agregata v surovi malti (1:2,99), malti za podlago (1:2,94) in zunanjem ometu (1:2,74). Z XRD so potrdili dominantne vrhove kalcita (razmik  $d \approx 0,303$  nm) s sekundarnimi silikatnimi in aluminatnimi fazami, medtem ko so FT-IR spektri pokazali karbonatne absorpcijske pasove pri  $\approx 1420$  cm<sup>-1</sup> in  $\approx 875$  cm<sup>-1</sup>, skupaj z organskimi podpisi, ki ustrezajo polisaharidom in amidnim skupinam. TG-DTA je pokazala veliko izgubo mase, 40–45 % med 600–780 °C, kar je posledica razpada CaCO<sub>3</sub>. Na SEM posnetkih so vidne kristalinične hidrirane faze C–S–H in portlandita, medtem ko je EDX analiza pokazala matrice, bogate s kisikom, z vsebnostjo Ca od 18 do 25 w% in vsebnostjo Si od 10 do 12 w%. S preiskavi izgube kisline so avtorji ugotovili stopnje raztapljanja od 7 do 9 w%, kar poudarja trajnost veziva. Barvni indeksi so kvantificirali tri različne pigmentne plasti: rdečo, bogato s hematitom, rumeno na osnovi svinca in ogljikovo črno. Ti rezultati skupaj dokazujejo uporabo homogenih mešanic in naprednih tehnologij na osnovi apna z organskimi dodatki, kar poudarja materialno dovršenost gradbenih praks 19. stoletja. Ta celovita, kvantitativno podprta raziskava ponuja kritičen vpogled v zgodovinske tehnologije izdelave malt in služi kot znanstvena podlaga za strategije ohranjanja indo-saracenskih spomenikov dediščine.

Ključne besede: dediščina 19. stoletja, zidane kupole, apnene malte, kemijska analiza, metode karakterizacije

## 1 INTRODUCTION

The Indian sub-continent has been endowed with a rich and diverse stock of cultural and architectural heri-

tage buildings, with a significant proportion of them constituting living monuments. India is a land of architectural marvels with some of the world's prominent religions tracing their roots deep in this country.<sup>1</sup> Over time, different dynasties that ruled or invaded India left their imprint on monuments and architecture. "However, the Mughals contributed significantly to India's Islamic architectural traditions, which later influenced heritage

\*Corresponding author's e-mail:  
p.thirumalini@yahoo.in (S. Thirumalini)



© 2026 The Author(s). Except when otherwise noted, articles in this journal are published under the terms and conditions of the Creative Commons Attribution 4.0 International License (CC BY 4.0).



**Figure 1:** The Madras High Court Building, Tamil Nadu, India

buildings such as the Madras High Court (Fig. 1), designed by British architects in the Indo-Saracenic style." Queen Victoria commissioned the construction, which began in 1888 and was concluded in 1892.<sup>1,2</sup> The Madras High Court complex, which spans 107 acres, is the second-largest judicial complex in the world after the Supreme Court of the United Kingdom, London).<sup>3</sup>

The Madras High Court is one of the oldest courts in India, located in Chennai, Tamil Nadu, with the latitude and longitude 13.08° N, 80.28° E across the coromandel coast of the Bay of Bengal, which was one of the most important provinces in India during the British colonial period. Chennai is the most significant cultural, economic, and educational center in South India. It has served as a substantial naval base and administrative center for centuries. The shelling on 22 September 1914, at the start of the first world war, severely damaged the court building. It remained one of the very few Indian buildings damaged by a German attack. Various cultures, including Portuguese and Dutch, further influenced its architecture.

The 40-meters-high red sandstone building with high ceilings, arches, ornamental tiling, and tall minarets was constructed with fired bricks and lime plaster in three layers. The present study was taken up to investigate the current status of ancient mortars and plasters of the madras Madras High Court dome. Modern analytical techniques including; X-Ray diffraction (XRD), Fourier transform-infrared spectroscopy (FT-IR), XRF-Chemical composition, Thermal-gravimetric analyses (TG-DTA), Scanning Electron Microscopy (SEM-EDX) were applied. The nature and the mix proportions of the mortar, their production technology and mineralogical formations were identified, as these aspects are essential for an understanding of the materials used and to inform the restoration of the dome structure with compatible materials and technologies. The nature and composition of the pigments used in ancient construction were also revealed

for a better match during simulation and replication work in safeguarding the rich heritage.

### ***1.1 Madras High Court Dome Mortar, Plaster, Pigments and its Current Situation***

The Madras High Court structure is holding up well, and there are no significant cracks on visual inspection. The longevity of this structure could be due to the raw materials used such as organic additives. H. Jedrzejska (1981) and L. Ventola et al (2011)<sup>1,2</sup> revealed that natural organics such as curd, jaggery, cactus extract, bel pulp (wood apple), lentils, oil of margosa, animal blood, wine, etc. had been used in ancient buildings to enhance their mechanical properties.<sup>4</sup> The use of organic materials and extracts of natural polymers from plants were used to bring positive changes in the fresh state and the hardened state properties of mortar.<sup>5,12</sup> The Madras Madras High Court used lime, sand, and a combination of organic materials to enhance the strength and durability of the structure. Even though the mortars of antiquated structures worldwide have been examined, limited works have been conducted on old Indian mortars, with significantly fewer publications.<sup>13,17</sup> Researchers like Chen Zhao et.al (2006), Rampazzi et.al (2016), and Thirumalini et al (2018) have been studying the characterization of ancient mortars and organic additives rich in fats, proteins, and carbohydrates, enhancing the binding capacity and reducing the cracking in plaster.<sup>18</sup> The various raw materials used in ancient mortars including organics make it challenging to understand the characteristics and application techniques.<sup>19</sup> The climatic conditions, humidity, and other environmental factors also play a vital role in the mortar's strength and durability, making it complicated to analyze ancient mortars.

The study of pigments is a broader topic because there is no boundary between the use of raw materials and production techniques. However, studies are limited to listing minerals used in different cultures and eras.<sup>20</sup>

New techniques and innovations continue to lead to the frequent discovery of natural minerals. However, over the ages, the production techniques and raw materials exploited have changed tremendously with little or no records available, hence making it very unlikely to re-engineer the materials. This work was carried-out, aligning to the framework of maintenance and restoration of Madras High Court in collaboration with Heritage Wing to analyze and re-engineer the damaged portions of the monuments as closely as possible to the original construction. A bilateral study was carried out to characterize the pigments and the mortar used in the Madras High Court building, using physio-chemical tests like acid loss analysis, grain size analysis and advanced analytical techniques like FTIR, SEM, XRF, XRD, TGA-DTA. The specific reason to restore the dome mortars is the structural damage and spalling of plasters on environmental exposure over centuries. The scientific investigation reports the type of raw material, binder to aggregate proportions by acid loss analysis, variety of pigment, and chemical composition to replicate a similar mortar to restore the Madras High Court building. This study serves as a benchmark for the state archaeology department and for modern conservators to document the ancient secrets that could be exploited and adopted for compatible restoration.

Pigment application is considered as one of the oldest ways to leave a mark (temporary or permanent) on any object. The architects and artisans of ancient times decorated and beautified buildings with extensive artwork that included precious and semi-precious stones<sup>3</sup> as well as natural pigments made from locally available materials. Properties such as setting time, light fastness, durability, mechanical characteristics, heat resistance, and soluble salt content are essential in pigmented mortar. The mortar's cohesion increases when pigments are used in the mortar mixture,<sup>4,5</sup> reducing the filler-material ratio used in the mix<sup>6,7</sup>. Lee et al.,<sup>8</sup> in a study on keyed concrete blocks using iron oxide pigment as the colorant, stated that the pigment/cement ratio must be less than 4%. Bruce and Rowe<sup>9</sup> used inorganic pigments as a colorant and found that these pigments are ten times more acceptable than cement and reported a decrease in the viscosity and thickness of mortars.

The Madras High Court building was decorated with permanent pigments that remain intact to date. A variety of colors is seen clearly in all the buildings. However, for the purposes of this study, the focus is specifically on one of the domes. Exposure of the domes to the environment, causes the pigments to fade, as **Figure 2** illustrates. The Madras High Court dome's murals are a blend of fresco (painting on the coating of wet plaster), secco (painting on the dry plaster), and stucco type (weather-proofing blend of anhydrous lime, marble powder, and glue). Generally, artists mix pigments in a paste or binder such as gum, mortar, or wax to embed them on a monument. The non-synthetic traditional pigments

used in the Madras High Court were primarily derived from plants, animals, and a combination of minerals. Pigments were synthesized using various chemicals and physical processes for manufacturing different colors, such as heating of yellow ochre to create red ochre.

The murals and domes were damaged due to various reasons such as the saline breeze (due to the proximity to the seashore), regional rough tropical weather, pigeon droppings, vibration and pollution due to heavy traffic, earlier unscientific interventions. The attractive murals on the Madras High Court domes, which are rare, are

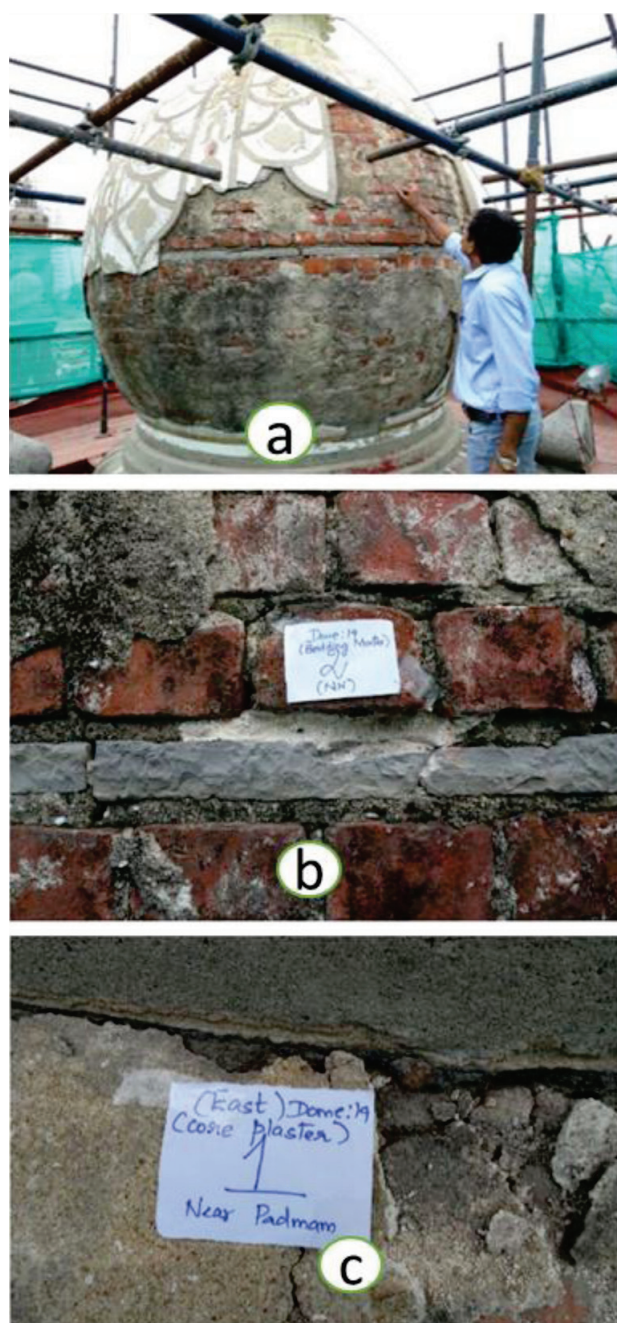


**Figure 2:** a) View of dome structure, b) Bedding and Bed raw mortar, c) Exterior plaster

**Table 1:** Sampling locations and their mortar typology specifications

I. No.	Location	No. of Samples per Dome	Sample weight (g)	Dimensions	Function of mortar	State of sample
1	North-East Dome	1	35.1	3 × 4 cm <sup>2</sup>	Bed Raw mortar	Powdered and pieces intact
2	West Dome No.19	1	48.2	5 × 6 cm <sup>2</sup>	Bedding mortar	Slightly damaged
3	South-East Dome	1	76.8	3 × 4 cm <sup>2</sup>	Exterior plaster	Slightly decolored

more than just paintings; they resemble the parquet work that adorns the Taj Mahal's monument. A well-refined colorful floral design pattern is carved in the lime base and inorganic pigmented material. The pigments are applied while the lime is wet, acting as a glue to secure the inserted inorganic pigments in place. The study focuses on identifying the minerals present in the pigments and their inorganic source by analytical characterization techniques, in order to enable the replication of similar pigments to regain the past glory of Madras High Court.

## 2 EXPERIMENTAL PART

### 2.1 Sampling of mortar

The sampling and collection of mortars, plasters and pigment layers from the domes were accomplished under the supervision and in conjunction with the State Archaeological Survey of Chennai and the Public Work Department (PWD) without causing any significant structural distress, as shown in Table 1. Three samples were taken at the following locations i) North East Dome (**Figure 2a**) ii) West Dome no 19 (West) (**Figure 2b**) and iii) the South-East Dome (**Figure 2c**) of the Madras High Court building. The locations were chosen to represent different orientations and exposure conditions of the High Court domes. The North-East dome provided a representative raw mortar sample with minimal prior intervention; the West Dome No. 19 was selected as it had previously reported structural repairs and hence provided bedding mortar; and the South-East dome, being highly exposed to saline breeze and weathering, was chosen for sampling the external plaster. This ensured that the collected samples captured a broad spectrum of original materials, environmental exposure, and degradation patterns across the monument. These samples were sieved through 75 µm, following Rilem TC-167 COM<sup>21</sup> to perform different analytical and chemical analyses.

### 2.2 Acid Loss Test

The acid loss test was performed to evaluate the binder to aggregate proportions. Mortar samples were gently crushed, guaranteeing that the aggregates were not pulverized. 30 g of crushed pieces of the samples were mixed with 200 mL of distilled water in a 500 mL measuring beaker. Then 30 mL of hydrochloric acid (0.1N) was added, stirred continuously for 60 min, and the filtrate was extracted. The filtrate was washed four

times with distilled water to prevent HCl attack. We adopted the 75-µm threshold to standardize the sample fineness for reproducibility and to ensure compatibility with XRF, XRD and FT-IR analyses. The remaining filtrate was weighed, and the total proportion (B/Agg) was given as equivalent to being standardized in the light of the binder content. The acid-loss test results provide information on the type of raw materials (binder, clay and aggregate grain size) used and their proportions.

### 2.3 Analytical techniques

X-ray fluorescence (XRF) evaluates the elemental bulk compositions of the finely ground mural pigment flakes and mortar samples <75 µm powder. Finely ground sample of 2–5 mg of was fed into Rigaku ZRX Primus II device mounted on the X-ray tube Rh anode 3 kW high-frequency inverter rotating at 30 min<sup>-1</sup>, with continuous scan 12-15 elements at 0.1–240 °C/min that registers the presence of elements under the nitrogen atmosphere.<sup>11,12</sup> Through the elemental analysis, the hydraulic and cementation Index was calculated as per the Eqn. (1) and (2) respectively.<sup>22,25</sup>

$$HI = (\%SiO_2 + \%Al_2O_3 + \%Fe_2O_3) / (\%CaO) \quad (1)$$

$$CI = (2.8 \times \%SiO_2 + 1.1 \times \%Al_2O_3 + 0.7 \times \%Fe_2O_3) / (\%CaO + 1.4 \times \%MgO) \quad (2)$$

The identification of lime was based on hydraulic index ranges, as developed by Taylor;

If

0.30 < HI < 0.50 – weakly hydraulic

0.50 < HI < 0.70 – moderately hydraulic

0.70 < HI < 1.10 – higher the index, more hydraulic properties

The classification of lime was based on cementation index as developed by Eckel;

If

CI < 0.15 – Fat lime

0.30 < CI < 0.50 – Slightly Hydraulic lime

0.50 < CI < 0.70 – Moderately Hydraulic lime

0.70 < CI < 1.10 – Eminently hydraulic lime

1.7 – Natural cement

The mineralogical phases were determined using X-ray diffraction with a Rigaku innovative lab II diffractometer, operating at 9 kW and a 9 mm beam size (slit aperture) according to the diffraction powder method. The sample holders were oriented in polymethyl methacrylate or Si of diameters 25 mm and 20 mm. The XRD patterns were obtained by scanning at the rate of

1°/min from 5° to 90° 2 $\theta$  position and at steps of 0.05° (2 h). The mineral phases were identified in each X-ray powder spectrum using the pan analytical high score 2.0 c software and the PDF 2/ICSD database. The Bruker Tensor 27IR, using KBr pellets, performed Fourier transform infrared spectroscopy (FT-IR) to measure the energy absorption. 5 mg of finely ground (<75  $\mu$ m homogeneously mixed powder), with 250 mg of KBr powder were mixed until the mixture had the consistency of fine flour and then pressed into a thin 15-mm diameter disc with infrared spectra obtained at 4000–400  $\text{cm}^{-1}$  range, with a resolution of 4  $\text{cm}^{-1}$  32 scans respectively.<sup>11,12</sup>

A Perkin Elmer Pyris-1 instrument was used to perform thermogravimetric analysis (TGA). The sample of 2 mg was placed in an alumina crucible. The temperature program ranged from room temperature to 1200 °C, at a heating rate of 10 °/min under the nitrogen (non-oxidizing agent) atmosphere. Field Emission Scanning Electron Microscopy (FE-SEM Carl Zeiss supra 55 coupled with energy-dispersive spectroscopy) was used to look at three different mortar samples and make morphological observations as well as semi-quantitative micro-chemical elemental analyses.<sup>19–21</sup> Three samples of bed raw, bedding mortar, and external plaster were sputter-coated with gold or palladium for 30 min in a vacuum evaporating system. The measurements were performed at variable spot sizes, ranging from 5 kx to 15 kV magnification, 20 mm WD, and EDS homogenous sample spot sizes of 10  $\mu$ m. EDX microanalysis used multipoint acquisition (8 spots per sample: 4 binders, 4 aggregate). Spots were chosen from a low-magnification survey image using a notional grid to ensure even coverage; each spot spectra was averaged to produce mean composition  $\pm$  SD reported in **Figure 9**.<sup>11,12,19–21</sup>

### 3 RESULTS

#### 3.1 Visual Examination

The mortar was dull white, which relates to the use of hydraulic lime during the construction of domes. The exterior plaster was affected by the environmental changes and found to be degraded, but the inner mortar was well-preserved and in a good condition.

From the visual observation it could be concluded that the collected bed raw sample had a rough and coarser appearance **Figure 3**. At the same time, the bedding mortar acts as a load-bearing material, revealing the binder-rich texture; the exterior plaster is a thin-lined mortar finished with a paint layer on its surface. Climate

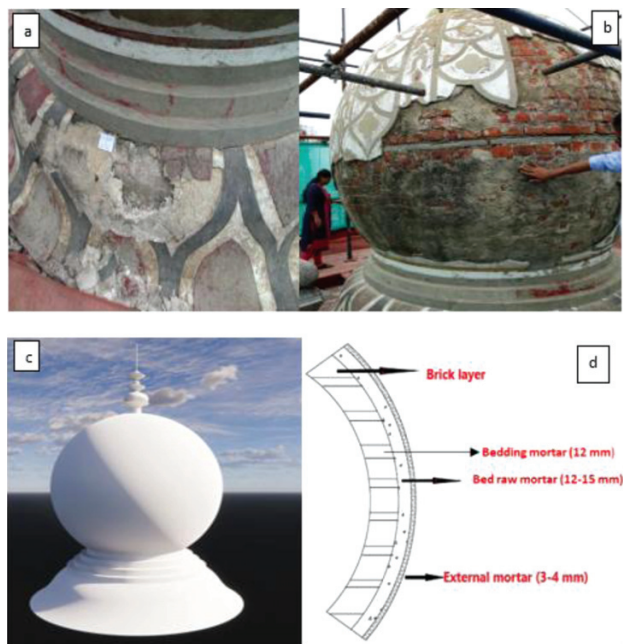


**Figure 3:** a) Pigment surface, b) Scaled pigment surface, c) Dome elevation, d) Dome plaster layers

conditions and environmental changes appear to have eroded the external mural surfaces over decades of severe exposure to the atmosphere.

The bed raw mortar sample was visualized with a Munsell color chart that displayed a high degree of cohesion, with color ranging from light yellow to brownish (Munsell 2.5 YR 6/3 to 10 YR 4/4 colors) as seen in **Figure 3** (a-c). Exterior pigment plaster displayed three different pigments—red, blue and black stains the third pigment (black) was too degraded for XRF quantification to decorate the domes with the Saracenic style of profiles as presented in **Figure 3d** and **Table 4**. Reference was made to "The new Munsell student color chart" to map the sample's color during the analytical experiment. This chart described the sample's shade, tinge, and color. The chemical composition of mural pigments indicated 21–55 % iron dominance in both red and black pigments, which gives a dark brown colour to the surface, and also copper of about 17–36 %, imparting the reddish-brown color to the profile.<sup>26,28</sup>

#### 3.2 Acid-Loss Test

The acid digestion analysis revealed that the binder to the aggregate ratio of bed-raw mortar is 1:2.99, bedding mortar is 1:2.74. an external plaster ratio of 1:2.96 (**Ta-**

**Table 2:** Binder-to-aggregate ratio of Madras High Court mortar samples

Type	Sample Wt. (g)	Acid Loss	Wt. after acid loss (g)	Wt. of sand retained (g)	Wt. of Binder (g)	B/Agg
Bed raw mortar	30.0	2.71	27.3	20.45	6.83	1:2.99
Bedding mortar	30.0	2.4	27.6	20.16	7.35	1:2.74
External plaster	30.0	2.15	27.5	20.82	7.03	1:2.96

ble 2). In chapter IV of "Ten books of Architecture", Vitruvius (1981) described how the best proportion adopted for hydraulic lime-based mortar is 1:3 for the highest carbonation. Also, mortar prepared with a 1:3 binder to aggregate ratio provides better workability and reduces pore spaces. Pliny the Elder stated in his manuscript, "Natural history", that when using lime and river or sea sand, 1:3 ratio should be adopted. Lanas and Alvarez<sup>29</sup> reported a binder to aggregate ratio of 1:3, which has the highest strength and reduced shrinkage cracks on the surfaces. Most researchers have experienced the mortar's performance by varying proportions and found that a 1:3 ratio gives better mechanical strength and improved durability.<sup>13</sup> In aged lime mortars, a low binder/aggregate ratio was preferred since a higher ratio could induce cracks. Non-aged lime mortars, on the other hand, require a high binder to aggregate ratio of 1:3 and do not show any early crack development.<sup>30</sup> Gameiro et al.<sup>31</sup> have noted that the higher aggregate proportion of 1:3 compared to 1:2 ratio has resulted in complete carbonation. The purpose of adopting the standard proportions was to sequester the external CO<sub>2</sub> to carbonate the surface, as the lime-based mortar is slow in hardening.<sup>32</sup> The re-carbonation process activates the internal mechanism to develop the early hydrated phases, which strengthen the mortar. The mortar typologies have played a significant role in enhancing workability, durability and mechanical stability. The 1:3 mortar typologies have demonstrated superior properties worldwide.

### 3.3. Particle size analysis of aggregate

The aggregate fractions from the acid-loss test were subjected to the particle size analysis, following IS 383-1970 standard test methods.<sup>33</sup> The raw materials were passed through a series of sieves ranging between 75 µm and 4.75 mm with optimum percentage retainment to evaluate the fineness modulus, as shown in **Table 3**. According to IS 383-1970,<sup>33</sup> the fineness modulus results for bedding mortar of 2.12 falls under zone 2, with the standard fineness modulus range being 2.1–2.5. The plaster fineness modulus results of 1.5, falls under zone 4 while the fineness modulus of hydrated lime range is 1.5–2.5. Fine sand was used for a better finish over the surfaces. The fineness modulus of sand in the range between 1.5 and 2.5 would be better for hydraulic

**Table 3:** Particle size distribution of acid-loss separated aggregates

Sieve size	Bedding Mortar (gm)	Plaster (gm)
4.75 mm	0	0
2.36 mm	0	1
1.18 mm	20	4
600 µm	24	4
300 µm	20	8
150 µm	20	4
75 µm	0	1
Pan	0	0

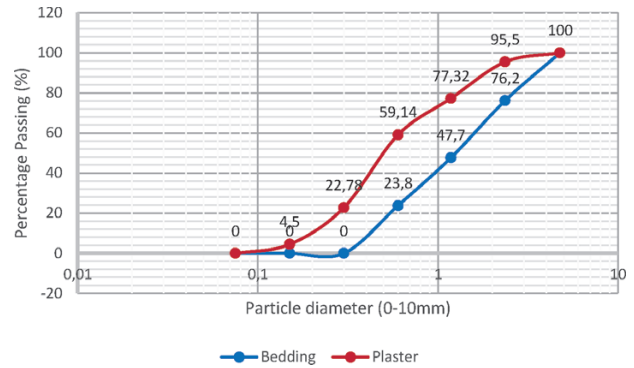


**Figure 4:** Particle size distribution on acid-loss separated aggregates

lime, while the sand made with fat lime would have a range between 2 and 3.<sup>34</sup>

#### 3.3.1 Grade characteristics of bedding mortar and plaster

The grain-size distribution of bedding mortar presented in **Figure 4** indicates that the bedding mortar aggregates used were uniformly graded, with the coefficient of uniformity (Cu) of sand being 3.06, falling below the range 4–6. Uniformly graded aggregates (IS: 383) will fill the voids between the paste. The curvature coefficient (Cc), which ranges from 0.60 to 1, indicates poor grading of the aggregates.<sup>33</sup> Similarly, the co-efficient of uniformity for aggregates used in the plaster is 2.93 (falling in the range 4–6), and the coefficient of curvature of plaster is 1.36 (falling in the range 1–3), indicating that the plaster is well graded. The bedding mortar aggregates show Cu = 3.06 and Cc ≈ 0.9. Under IS:383 grading zones this places the sand in zone 2 (coarser sand). A Cu of ≈3 indicates moderate uniformity rather than the elevated values (>6) typically associated with well-graded sands for specific structural uses; we therefore characterize the bedding sand as moderately uniform/less well-graded rather than well-graded.<sup>33,34</sup>

### 3.4 Chemical composition

#### 3.4.1 Dome Pigments

The separation of pigment from binder was achieved in accordance with RILEM TC167.COM, through an acid-loss test. A solution of 1N HCL dissolves the binder part by separating the aggregate fraction and pigment layer. **Table 4** presents the chemical composition of plaster pigments. The red stain pigment comprises iron oxide at around 53 % and copper oxide at around 17 %. That imparts a reddish-brown color along with lead and zinc, ranging around 9–14 %. The zinc white has induced the property to accelerate the light fading process of paints that contains the organic pigments and moderately absorbs the amount of aqueous solution from the organics.<sup>35</sup> Red lead blackening is commonly associated with interaction with reduced sulfur species (e.g., H<sub>2</sub>S) and atmospheric pollutants, leading to formation of PbS

or lead carbonates; this mechanism is consistent with the partial blackening observed on the pigments. The XRF analysis on the paint layer reported the presence of Cu in the range of 17 % in the red pigment sample and 36.24 % in the blue-black pigment sample. The analysis of the red pigment sample shows that the Fe and Cu at around 62–65 %, impart a red stain to the surface. Cuprite is a copper oxide ( $\text{Cu}_2\text{O}$ ) recognizable by its reddish-brown color. The formation of cuprite depends on the environment. If directly exposed to the atmosphere, copper and its alloys form a thin corrosion layer on the surface.

If the structure is exposed to high levels of humidity, cuprite formation can be favored by the presence of chlorides. The presence of cuprite has a significant impact on the degradation of paint layers, as more complex products can be formed.<sup>36</sup> The presence of minor traces of calcium, silica, titanium, and sulphur at less than 5 % level, act as a primer and improve the particle's accumulation in the pigment. Moreover, black paint made of carbon black was used to outline the patterns of the dome paintings. It is also seen that the red lead was partially blackened, likely due to the action of air pollutants.<sup>35,36</sup> The composition of the blue-black pigment showed a significant amount of Cu at approximately 36 %, and Pb at 17 %, suggesting that the dome's design utilized the ultramarine blue color. This ultra-marine blue is often combined with lead white to obtain different shades. Hofmann et al. 2003<sup>37</sup> reported the presence of aluminum and silicon indicating the presence of ultramarine blue ( $\text{Na}_7\text{Al}_6\text{Si}_6\text{O}_{24}\text{S}_3$ ) while high intensities of lead (Pb) point to the use of lead white. A high Ca percentage of 13 % has induced the pigment to adhere and is responsi-

ble for the white color with traces of Si, S, and Ti to improve the pigment's viscosity.<sup>38,39</sup>

**Table 4:** Chemical composition of pigments sampled from the dome

Sample w/%/Mass	Si	S	Ca	Ti	Fe	Cu	Zn	Pb
Red Pigment	0.59	0.29	4.12	2.331	53.14	17.04	9.09	13.37
Blue-Black Pigment	1.06	0.44	13.02	1.58	21.24	36.24	9.86	16.52

### 3.4.2 Dome Mortars

The chemical analysis performed on dome mortars presented in **Table 5** confirms the major element being Ca at around 65–67 %, and the presence of ceramic elements of  $\text{SiO}_2$  at 22–25 % in the various spots of extricated dome mortar samples. This confirms that the sample is primarily hydraulic with the CI and HI index range between 0.7 and 1.1, Taylor et al (1905). The calcium content was reported at a maximum, whereas the Mg content was present in minor traces in all the mortar samples. The XRD and FT-IR analysis confirmed no significant dolomite peaks (e.g., dolomite  $2\theta \approx 30.9^\circ$ ,  $33.0^\circ$  in XRD; FT-IR bands near  $730\text{--}730\text{ cm}^{-1}$  /  $745\text{ cm}^{-1}$  diagnostic) were observed above detection limits in our XRD/FT-IR patterns. However, the presence of a small quantity of MgO would resist the drying shrinkage and contributes to better carbonation action. Minor MgO ( $\approx 1\text{--}2\%$ ) can reduce drying shrinkage via formation of slowly reacting Mg-phases that densify the matrix and by promoting heterogeneous nucleation of carbonate phases, thus aiding long-term carbonation and microstructural stability.<sup>18–21</sup>

**Table 5:** XRF elemental composition of sampled mortars.

Sample w/%/Mass	Si	Al	Mg	Ca	Ti	Fe	Sr	Pb	S	LOI (%)	HI	CI
Bed raw mortar	25.8	8.3	1.47	67.16	0.12	3.62	0.23	1.32	0.53	3.58	0.72	0.89
	27.2	7.9	1.95	65.15	0.1	3.44	0.22	1.45	0.45	3.44	0.74	0.91
	24.6	8.1	1.55	63.5	0.14	2.89	0.25	1.3	0.48	3.25	0.70	0.88
Mean	25.8	8.1	1.65	65.27	0.12	3.31	0.23	1.35	0.48	3.42	0.72	0.90
SD	1.3	0.2	0.25	1.83	0.02	0.38	0.01	0.08	0.04	0.16	0.1	0.1
SE	0.43	0.06	0.08	0.61	0.006	0.12	0.005	0.02	0.01	0.05	0.03	0.02
Bedding mortar	24.13	8.1	2.04	64.9	0.15	3.22	3.82	—	—	1.58	0.76	0.96
	22.45	7.95	1.95	63.8	0.22	3.4	3.35	—	—	1.25	0.74	0.97
	25.15	8.22	2.1	64.3	0.18	3.1	3.85	—	—	1.46	0.72	0.93
Mean	23.91	8.09	2.03	64.3	0.18	3.24	3.67	—	—	1.43	0.74	0.95
SD	1.36	0.13	0.07	0.55	0.03	0.15	0.28	—	—	0.16	0.1	0.1
SE	0.45	0.04	0.02	0.18	0.01	0.05	0.09	—	—	0.05	0.02	0.03
External plaster	22.34	7.95	1.68	65.7	1.46	2.36	4.13	1.25	—	1.08	0.77	1.03
	21.55	7.45	1.65	64.8	1.44	2.1	3.85	1.1	—	0.98	0.72	1.05
	22.1	7.8	1.55	65.1	1.35	2.24	4.1	1.2	—	1.04	0.73	1.04
Mean	21.9	7.73	1.62	65.2	1.41	2.23	4.67	1.1	—	1.03	0.75	1.04
SD	0.40	0.25	0.06	0.45	0.05	0.13	0.15	0.07	—	0.05	0.2	0.02
SE	0.13	0.08	0.02	0.15	0.01	0.04	0.05	0.02	—	0.01	0.01	0.03

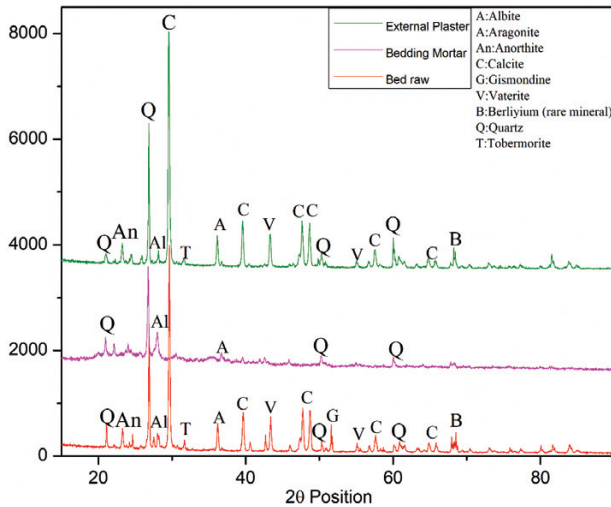


Figure 5: X-Ray diffraction patterns of: a) Bed raw, b) Bedding mortar, c) External lime plaster

### 3.5 Mineralogical analysis

#### 3.5.1 XRD analyses

The XRD results in **Figure 5** (a-c) reveal the principal peaks to be calcite, silica, and quartz in all the mortar samples. Besides the presence of high-intensity peaks of calcite, the results also show other polymorphs of carbonates in traces like vaterite and aragonite in the 150-year-old bed-rw mortar sample. These observations agree with the minor trace of aragonite spectral FT-IR peaks at 856  $\text{cm}^{-1}$  and 1475  $\text{cm}^{-1}$ , respectively. The presence of calcium aluminates (gismondine and anorthite) peaks indicates the quick hydrated phases formed without portlandite or free calcium<sup>40,41</sup> (**Figures 5** a-c). High intensity peaks of quartz, cristobalite, albite, anorthite with minor traces of calcite and metastable vaterite peaks were observed in the XRD analysis of bedding mortar. That agrees with the 1068  $\text{cm}^{-1}$  silica peak in FT-IR analysis. The chemical composition (**Table 5**) of bedding mortar also revealed a high-intensity silica percentage (22–25 %), indicating the lime mortar’s hydraulicity, confirmed with the moderate intensity of O-H peaks observed at 3304  $\text{cm}^{-1}$  and 1605  $\text{cm}^{-1}$  in the FTIR analysis. In **Figure 5c**, the XRD patterns of external lime plaster revealed high-intensity calcite and quartz peaks with traces of aragonite and vaterite, indicating the formation of hydrated phases. Portlandite peaks are absent. Traces of Wollastonite ( $\text{CaSiO}_3$ ) were identified through XRD analysis, attributing these peaks to the residues of brick aggregates from the external surface of the dome. The wollastonite appearance reflects that the lime has been over calcined at  $> 848^\circ\text{C}$ , agreeing with 26.95 % mass loss observed in **Figure 7c**. The Wollastonite contains a small amount of iron, magnesium and manganese, substituting for calcium. The presence of Wollastonite can be achieved during the extraction of bed raw mortar attached to the masonry units. It can be considered a ther-

mal indicator with a calcined temperature peak observed over 850  $^\circ\text{C}$ . The predominant peaks of calcite and quartz in the absence of portlandite, indicate that the entire surface is carbonated<sup>41,42,43</sup>.

#### 3.5.2 FT-IR Interpretation

The FT-IR absorption analyses presented in **Figure 6a** indicate the formation of several spectral peaks associated with calcite vibrations observed at (1421, 874 and 712)  $\text{cm}^{-1}$ , quartz peak around (645 and 1068)  $\text{cm}^{-1}$  and the clay mineral peaks observed at (3779 and 964)  $\text{cm}^{-1}$ , respectively. Generally, the stretching and bending absorbance signals at (2921 and 2854)  $\text{cm}^{-1}$ , respectively, suggest the CH bond. The presence of minor traces of C-H polysaccharide vibration observed at 2926  $\text{cm}^{-1}$  in-

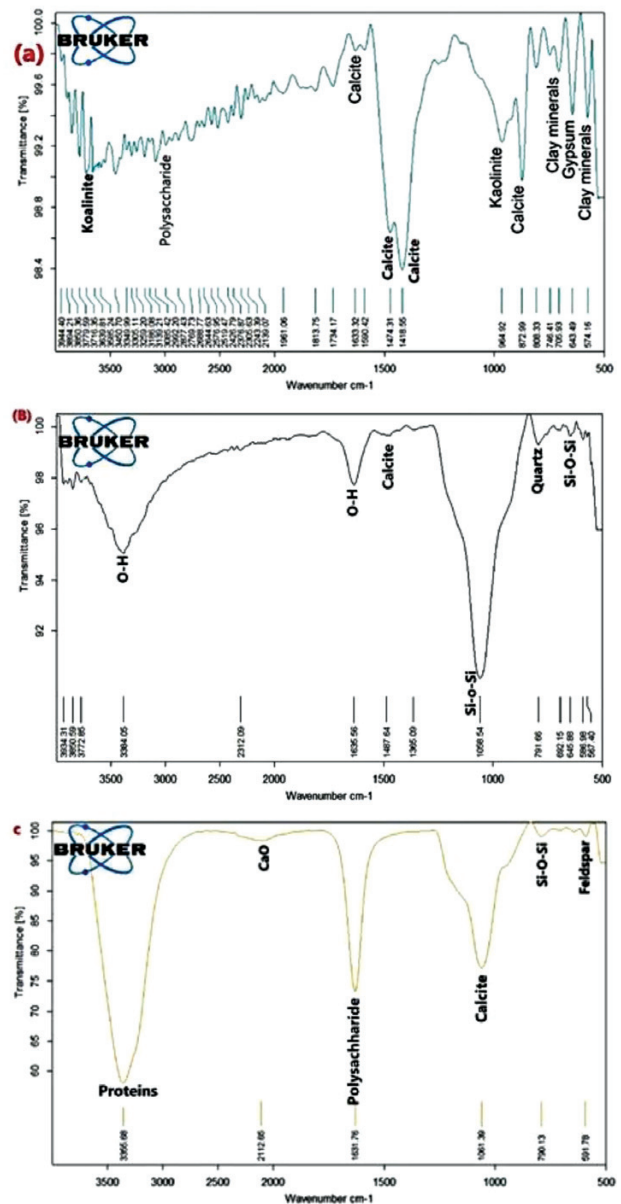


Figure 6: FT-IR for samples: a) Bed raw Mortar, b) Bedding mortar, c) External Plaster

indicates organics added in the lime mortar in production during construction<sup>43,44</sup>. The addition of organics led to the observation of traces of carbonate polymorphs like aragonite and vaterite (**Figure 6a** and **6b**). The bedding mortar FT-IR sample reveals the high-intensity quartz and silica-containing minerals observed at 1060 cm<sup>-1</sup> and 791 cm<sup>-1</sup>. This observation indicates the addition of high argillaceous minerals with a low fraction of binder phases observed at 1421 cm<sup>-1</sup> in agreement with minor traces of calcite peaks in the XRD bedding mortar sample. The spectroscopic results reported in **Figure 6c** in-

dicating the high-intensity calcite, silica, and feldspar peaks observed at 1071 cm<sup>-1</sup>, 790 cm<sup>-1</sup> and 591 cm<sup>-1</sup>.<sup>44</sup> Rampazzi et al. (2016) reported the presence of C-H polysaccharide and proteinaceous peaks at 3366 cm<sup>-1</sup> and 1631 cm<sup>-1</sup>, respectively. The FTIR spectra confirmed that aliphatic C-H stretches around 3000–2800 cm<sup>-1</sup> and clay impurities at 3650 cm<sup>-1</sup>. The peaks observed in all dome mortars represent the predominant formation of carbonates, clay minerals, and organic additives and are consistent with the results of the XRD analysis.<sup>45</sup>

### 3.5.3 Thermal analyses

**Figure 7** (a-c) presents the results of the TG-DTA analysis. Moreover, the thermal analysis reports the absorbed water (hygroscopic water) in the temperature range up to 120 °C, the gypsum dehydration which occurs between (120 and 200) °C, the structurally bound water to the hydraulic components in the temperature range 200–600 °C, and the calcite decomposition above 600 °C.<sup>41–43</sup>

The bed raw TG-DTA analysis in **Figure 7a** revealed the dehydration mass loss of 1.96 %, which is less than 3 % as for typical lime mortar. The second stage refers to the structurally bound water with the loss of the hydraulic component observed at around 2.01 %, with endothermic calcite decomposition at 823 °C with a mass loss of about 26.95 % subjected to complete release of CO<sub>2</sub>.<sup>44,45</sup> The CO<sub>2</sub>/H<sub>2</sub>O ratio of bed raw mortar ranged at 6.78 up to 10 for the hydraulic mortar. Predominantly the

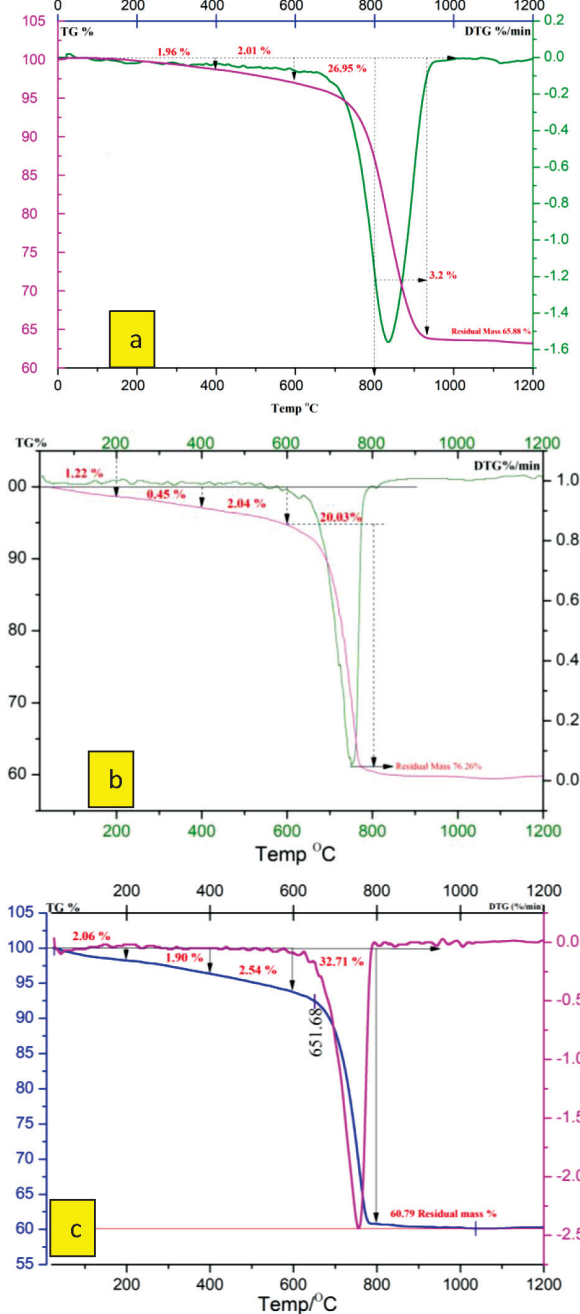


**Figure 7:** TGA and DTA graphs of: a) Bed raw, b) Bedding mortar, c) External plaster

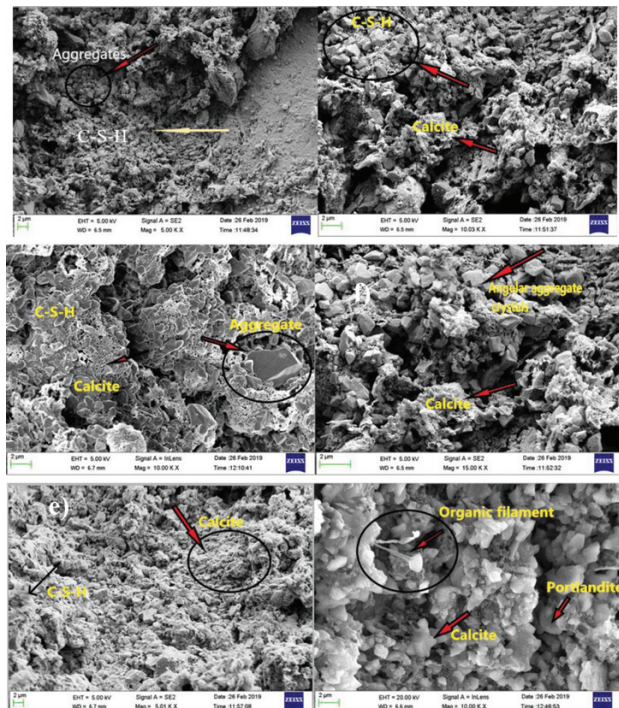


**Figure 8:** (a-b) Bed raw mortar images with C-S-H and C-H gel formation (c-d). Bedding mortar images showing carbonate flakes carpeted over angular shaped aggregate crystals. (d-e). Images show well compact amorphous calcite and quartz.

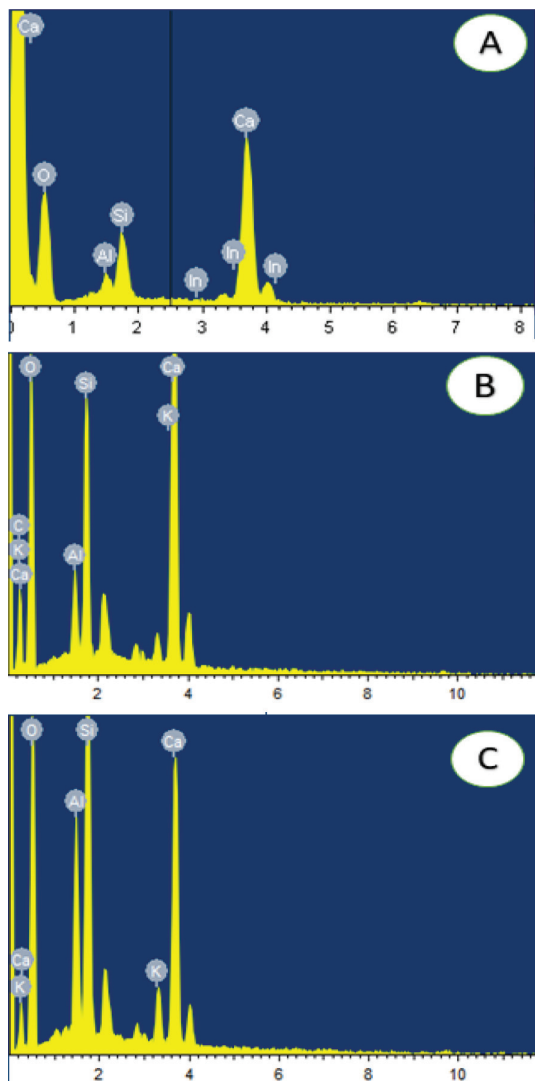


**Figure 9:** EDX spectrum of Dome mortars: a) Bed raw mortar, b) Bedding mortar sample, c) External plaster

decarbonation in the lime mortar takes place between (600 and 800) °C. But in the bed raw mortar, the XRD analysis revealed the presence of a Wollastonite peak with the melting point over 1500 °C. The TGA analysis also signaled the shift in the decarbonation over 800 °C with a loss of 27 %, as shown in **Figure 7**. The Wollastonite contains a small amount of iron, magnesium and manganese, substituting for calcium. The calcite decomposition was observed at 823 °C with the formation of hydrated phases of CSH and CH in agreement with similar calcitic and clay mineralogical peaks observed in the FT-IR and XRD analyses. Bedding mortar and external lime plaster resulted in the structurally bound mass loss of around (2.49 and 4.44) %, as shown in **Figure 7** (b-c), with high mass loss observed in exterior lime plaster, in the presence of organics decomposition (around 1.90 %) in association with organic spectral peaks, noted in FT-IR.<sup>45</sup> Calcite decomposition was observed, with an endothermic peak at 780 °C with a mass loss of around

20.03 % and 32.71 %, indicating the CO<sub>2</sub>/H<sub>2</sub>O factor of 9.77 and 7.36 (less than ten), resulting in the take up of hydraulic lime in the production of traditional mortar. According to the analysis of all the mortar samples, there is no clear evidence of the carbonate polymorphic peaks of aragonite and vaterite. The high-intensity mass loss observed in external plaster indicates the highly carbonated phases in the formation of calcite.<sup>45,46</sup>

#### 3.5.4 FESEM-EDX analyses

The magnification range of 5 k× and 10 k× for bed raw mortar, and of 10 k× and 15 k× for external plaster, was adopted in the SEM observations. Hence the overall range was between 5 and 15 k×. EDX spectra were captured at a similar location, as shown in **Figures 8** and **9**. The morphological observation gave valuable information about dome mortar samples such as binders, aggregates and reaction compounds, and also in identifying their sizes, forms, textures, and distribution matrix. The bed-row samples in **Figure 8** (a-b) evidenced calcite crystalline formed phases with distinct hydraulic compounds (CSH and CH). Calcium silicate hydrates and calcium hydrates have modified the lime mortar mix's texture and microstructure, resulting in increased hydraulic properties and enhanced mechanical characteristics.<sup>46,47</sup>

Furthermore, CH contributes to the mix's compactness and high flexibility. The EDX spectrum in **Figure 9a** shows that the major elements (Ca, Si) and typical K-feldspar are present in the sample, indicating the carboniferous calcite formation. **Figure 8** (c-d) revealed high siliceous and calcareous compounds distributed evenly in forming the calcium silicates. These are in good agreement with XRD, FT-IR, and chemical composition observations.<sup>45,48,49</sup> **Figure 9** (a-c) shows widespread calcite crystals with organics playing a vital role in forming hydrated phases and resisting environmental degradation. The presence of both amorphous and crystalline phases in the mortar samples contributes to the self-healing of lime mortar, enhancing its durability. The EDX spectrum in **Figure 9c** indicates high calcium and lower intensity silica and alumina along with lanthanides (rare-earth elements) ranging around 3.58 % present in the sample.<sup>46</sup> Dome mortar samples with more oxygen and less carbon, suggest that high calcite has formed.

On the other hand, high carbon and less oxygen resemble the low calcite formed in the external plaster sample. As indicated in **Figure 9** (a-c) dome mortar samples with more oxygen and less calcium implies high calcite formations. However, this observation also resembles the low calcite formed in the external plaster sample. All the mortars' matrices are, obviously, rich in calcium and silicates, as can be seen from the XRD analysis, where the presence of pure calcite and calcite-silicate limes was identified.<sup>19,38</sup>

## 5 DISCUSSION

### 5.1 Recipe for Dome mortars

The physio-chemical and analytical techniques show that the lime used is hydraulic with a binder-to-aggregate ratio of 1:2.75–3. The particle size of the aggregate falls under zone 2 IS 2386 (Part 1):1963 for coarse sand, which is suitable for the bedding mortar. The external plaster aggregate is well-graded and falls under zone 4 with a reduced grain size between 1.18  $\mu\text{m}$  and 600  $\mu\text{m}$ . The bedding mortar layer is proportioned with 1 part of lime to 2.75, with aggregates passing 2.36 mm. Given the organic peaks observed through FTIR analysis, it can be suggested that the Indian organics, namely Jaggeri and Kadukkai, were used, subjected to fermentation at the ratio of 5 % of weight to 1 liter of water and allowed for semi aerobic reaction in atmosphere for 14 days.<sup>48–52</sup> The justification for the traditional practice and reason behind organic fermentation are scientifically unknown. Still, the recent research and scientific study on materials have reported the fermentation action performed on Indian organics is intended to break the organic substrate into simple monomers forming the alcoholic solution. The fermented water reacts with the lime, forming calcium alkoxide, increasing the formation of hydration products and increasing the carbonation.<sup>53</sup>

### 5.2 Dome Pigment

Based on the analytical interpretation conducted, it can be noted that the pigment is rich in iron oxide, cuprous oxide and zinc, imparting the reddish-brown color. It is noted that 53.14 % of Fe, 17.04 % of Cu and 9 % Zn are mixed to formulate the red pigment and blue-black pigment with 16.52 % Pb, 21 % of Fe, and 36.24 % of Cu, responsible for the ultramarine blue-black color. The addition of zinc between (9–15 %) protects the pigment from fading.<sup>54</sup>

## 6 CONCLUSIONS

This study provides a comprehensive scientific characterization of the Madras High Court dome mortars and pigments, enabling restoration strategies rooted in historical accuracy. Analyses confirm the original use of hydraulic lime mortars with a binder-to-aggregate ratio close to 1:3, ensuring durability and breathability, while pigment characterization revealed iron- and copper-based formulations with minor zinc components, guiding authentic color replication. Environmental exposure and earlier unscientific repairs have degraded the external plaster layers, highlighting the need for compatible materials.

The restoration must prioritize material compatibility over modern Portland cement, which risks chemical and physical incompatibility. Practical restoration recommendations include using lime-based mortars with a 1:3 binder-aggregate ratio matching historical composition,

employing graded aggregates (Zone 2 for bedding, Zone 4 for plasters) for structural and aesthetic fidelity, and recreating pigments using iron-copper formulations with protective zinc additives for longevity, while avoiding modern synthetic pigments unless laboratory tests confirm compatibility.

Repair mortars should match the original particle-size distribution and hydraulic properties (HI  $\approx$  0.7–0.8) to prevent differential mechanical behavior, and Portland cement mortars should be avoided.

For pigment replication, inorganic pigment formulations matching XRF compositions must be used, while thermally altered zones showing Wollastonite traces require structural testing before large-scale interventions.

Prior to repair, friable external plasters should be consolidated with breathable lime-compatible consolidants, followed by sacrificial protective coatings where exposure necessitates, with all interventions thoroughly documented for long-term conservation records. Restored areas must be monitored using hygrothermal sensors to ensure material compatibility and durability over time.

Additionally, training local artisans in traditional lime techniques, integrating preventive maintenance programs, conducting structural assessments in vulnerable areas, and implementing periodic inspections will collectively safeguard the monument's structural integrity and cultural heritage for future generations.

### Acknowledgement

The authors would like to thank and extend their gratitude to Heritage Wing, Madras High Court headed by Mr Sivana, and the Public Works Department. We also extend our sincere thanks to the School of Civil Engineering, Vellore Institute of Technology, for supporting and motivating this research work.

### Data availability statement

No data associated in the manuscript.

### Ethics Approval and Consent to Participate

Not applicable.

### Consent for Publication

The authors grant their full consent for the publication of the above material, which is the property of the authors.

### Competing Interests

The authors declare no conflict of interest. The funders had no role in the design of the study; in the collection, analyses, or interpretation of data; in the writing of the manuscript; or in the decision to publish the results.

## 5 REFERENCES

- <sup>1</sup> Bandyopadhyay, R., Morais, D. B., & Chick, G. Religion and identity in India's heritage tourism. *Annals of Tourism research*, 35 (2008) 3, 790–808
- <sup>2</sup> History of Madras Madras High Court. Madras Madras High Court. Archived from the original on 11 March 2014. Retrieved 25 April 2014
- <sup>3</sup> Madras Madras High Court. BSNL. Archived from the original on 30 January 2012. Retrieved 2 March 2012
- <sup>4</sup> Dirlam, D. M., Rogers, C. L., & Weldon, R. Gemstones in the era of the Taj Mahal and the Mughals. *The Quarterly Journal of the Gemological Institute of America*, 55 (2019) 3, 294–319
- <sup>5</sup> Hoffmann, D. L., Standish, C. D., García-Díez, M., Pettitt, P. B., Milton, J. A., Zilhão, J., ... & Pike, A. W. (2018). U-Th dating of carbonate crusts reveals Neandertal origin of Iberian cave art. *Science*, 359(6378), 912–915
- <sup>6</sup> Bruce, S. M., & Rowe, G. H. (1992). The influence of pigments on mix designs for block paving units. In *Proceedings of the 4th International Conference on Concrete Block Paving* (Vol. 2, pp. 117–124)
- <sup>7</sup> L'opez, J. M. Tobes, G. Giaccio, and R. Zerbino, Advantages of mortar-based design for coloured self-compacting concrete, *Cement and Concrete Composites*, vol.31, no.10, pp.754–761, 2009
- <sup>8</sup> M. Collepardi and A. Passuelo, The best SCC: stable, durable and colourable, in *Proceedings of the 4th International ACI/CANMET Conference on Quality of Concrete Structures and Recent Advances in Concrete Materials and Testing—FurnasCentraisElétricasSA*, P. Helene, T. C. Holland, E. Pazzini, and R. Bittecourt, Eds., Civil Engineering Technological Center, Goibnia, Brasil, 2005
- <sup>9</sup> V. Corina desi, S. Monosi, and M. L. Ruello, Influence of inorganic pigments' addition on the performance of coloured SCC, *Construction and Building Materials*, vol.30, pp.289–293, 2012
- <sup>10</sup> S. M. Bruce and G. H. Rowe, The influence of pigments on mix designs for block paving units, in *Proceedings of the 4th International Conference on Concrete Block Paving*, vol.2, pp. 117–124, Auckland, New Zealand, 1992
- <sup>11</sup> Thirumalini S, Ravi R, Sekar S, Nambirajan M. Knowing from the past—ingredients and technology of ancient mortar used in vadakumnathan temple, tirussur, kerala, india. *Journal of Building Engineering* 2015; 4:101–12
- <sup>12</sup> Ravi R, Selvaraj T, Sekar S. Characterization of hydraulic lime mortar containing 18 opuntia Ficus- Indica as a bio-admixture for restoration applications. *International Journal of Architectural Heritage* 2016;10(6):714–25
- <sup>13</sup> R. Malinowski, Ancient mortars and concretes. durability aspects. in: *Mortars, Cements and Grouts Used in the Conservation of Historic Buildings*. Symposium, Rome, 3–6 Nov. 1981. Mortiers, ciments et coulis utilisés dans la conservation des bâtiments historiques', Symposium, Rome 3–6 Nov. 1981, Iccrom, 1982, pp. 341–350
- <sup>14</sup> Pilot Study – Conservation of Historic Brick Structures, Symposium, 25th – 27th October, 1991, Umweltbundesamt, Berlin, Germany, pp. 75 – 92
- <sup>15</sup> L. Sbordoni-Mora, Les matériaux des enduitstraditionnels, in: *Mortars, Cements and Grouts Used in the Conservation of Historic Buildings/Mortiers, ciments et coulis utilisés dans la conservation des bâtiments historiques*, ICCROM, 1981, pp.375–383
- <sup>16</sup> Lanás, J., Bernal, J. P., Bello, M. A., & Galindo, J. A. (2004). Mechanical properties of natural hydraulic lime-based mortars. *Cement and Concrete Research*, 34(12), 2191–2201
- <sup>17</sup> D. Carran, J. Hughes, A. Leslie, C. Kennedy, A short history of the use of lime as a building material beyond Europe and north America, *Int. J. Archit.Herit.* 6 (2) (2012) 117–146
- <sup>18</sup> Singh, M., Kumar, S. V., Waghmare, S. A., & Sabale, P. D. (2016). Aragonite–vaterite–calcite: Polymorphs of CaCO<sub>3</sub> in 7th century CE lime plasters of Alampur group of temples, India. *Construction and Building Materials*, 112, 386–397
- <sup>19</sup> Thirumalini, S., Sekar, S. K., Bhuvaneshwari, B., & Iyer, N. R. (2015). Bio-inorganic composites as repair mortar for heritage structures. *J. Struct. Eng.*, 42, 294–304
- <sup>20</sup> Ioanna Papayianni, Vasiliki Pachtá, Maria Stefanidou, Analysis of ancient mortars and design of compatible repair mortars: the case study of Odeion of the archaeological site of dion, *Constr. Build. Mater.* 40 (2013) 84–92
- <sup>21</sup> B. Middendorf, J.J. Hughes, K. Callebaut, G. Baronio, I. Papayianni, Investigation methods for the characterisation of historic mortars – Part 2: chemical characterisation, *RilemTC-167-COM*, *Mater. Struct.* 38 (2005) 771–780
- <sup>22</sup> S. Pavia, B. Toomey, Influence of the aggregate quality on the physical properties of natural feebly-hydraulic lime mortars, *Mater. Struct.* 41 (3) (2008) 559–569
- <sup>23</sup> Taylor H. *Cement chemistry* 1997
- <sup>24</sup> Eckel EC. *Clements, Limes and Plasters: Their Materials, Manufacture and Properties*. 1922
- <sup>25</sup> Toprak G. Characteristics of limes produced from marbles and limestones. Master's thesis; Izmir Institute of Technology; 2007
- <sup>26</sup> A.H. Munsell, *Color soil charts*, 1994
- <sup>27</sup> Munsell Color (1994). *Munsell Soil Color Charts* (1994). Rev. edn. Mabeth Division of Kollmorgen Instruments, New Windsor, NY
- <sup>28</sup> C. Rispoli et al., The ancient pozzolanic mortars of the Thermal complex of Baia (Campi Flegrei, Italy), *J. Cult. Herit.*, vol. 40, pp. 143–154, 2019
- <sup>29</sup> Lanás J, Alvarez JI (2003) Masonry repair lime-based mortars: factors affecting the mechanical behavior. *Cem Concr Res* 33: 1867–1876
- <sup>30</sup> K. Elert, C. Rodríguez-Navarro, E.S. Pardo, E. Hansen, O. Cazalla, Lime mortars for the conservation of historic buildings, *Stud. Conserv.* 47 (1) (2002) 62–75
- <sup>31</sup> Gamberio, P. Santos Silva, J. Faria, T. Grilo, R. Branco, A. Velosa Veiga, Physical and chemical assessment of lime–metakaolin mortars: influence of binder:ag-gregateratio, *Cem. Concr. Compos.* 45 (2014) 264–271
- <sup>32</sup> Nijland, T., Larbi, J., van Hees, R.P.J., Lubelli, B., de Rooij, M. (2007). Self-healing phenomena in concrete and masonry mortars, in *Proceedings of the 1st International Conference on Self Healing Materials*, Noordwijk, The Netherlands, 2007, 18–20 April 2007
- <sup>33</sup> IS: 383, Specification for coarse and fine aggregates from natural sources for concrete, BIS, New Delhi, 1970
- <sup>34</sup> Interior, U. S. D. of the B. of R. (1998). *Earth manual*. Revised, First Edition. Washington, DC, 348
- <sup>35</sup> Fancy, S. F., Lau, K., Sabbir, M. A., & DeFord, D. (2019, March). Extended Connectivity of Zinc Pigments to Provide Enhanced Galvanic Coupling by Partial Replacement with Nano-particles. In *CORROSION 2019*. One Petro
- <sup>36</sup> H. Karimy and P. Holakooei, Analytical studies leading to the identification of the pigments used in the Pi'r-i Hamza Sabzpu'sh Tomb in Abarqu', Iran: A reappraisal, *Period. di Mineral.*, vol. 84, no. 3A, pp. 389–405, 2015
- <sup>37</sup> Veneranda, M. (2017). Development of novel procedures for the preservation of archaeological irons and mural paintings (Doctoral dissertation, Universidad del País Vasco-Euskal Herriko Unibertsitatea)
- <sup>38</sup> Hofmann, C., Rabitsch, S., Malissa, A., Aceto, M., Uhlir, K., Griesser, M., ... & Fenoglio, G. (2020). The miniatures of the Vienna Genesis: Colour identification and painters' palettes. *The Vienna Genesis*; Hofmann, C., Ed.; Böhlau Verlag: Vienna, Austria, 201–246
- <sup>39</sup> S. A. Yildizel, G. Kaplan, and A. U. Öztürk, Cost optimisation of mortars containing different pigments and their freeze-thaw resistance properties, *Adv. Mater. Sci. Eng.*, vol. 2016, no. February, 2016
- <sup>40</sup> T. S. Nayar, S. Binu, and P. Pushpangadan, Uses of plants and plant products in traditional Indian mural paintings, *Econ. Bot.*, vol. 53, no. 1, pp. 41–50, 1999
- <sup>41</sup> S. Thirumalini, R. Ravi, S. K. Sekar, and M. Nambirajan, Knowing from the past – Ingredients and technology of ancient mortar used in

- Vadakumnathan temple, Tirussur, Kerala, India, *J. Build. Eng.*, vol. 4, no. August 2017, pp. 101–112, 2015
- <sup>42</sup> R. Ravi, S. Thirumalini, and N. Taher, Analysis of ancient lime plasters – Reason behind longevity of the Monument Charminar, India a study, *J. Build. Eng.*, vol. 20, no. July 2017, pp. 30–41, 2018
- <sup>43</sup> S. Pradeep and T. Selvaraj, Identification of Bio-Minerals and Their Origin in Lime Mortars of Ancient Monument: Thanjavur Palace, *Int. J. Archit. Herit.*, vol. 0, no. 0, pp. 1–11, 2019
- <sup>44</sup> C. Manoharan, R. Venkatachalapathy, S. Dhanapandian, and K. Deenadayalan, FTIR and Mössbauer spectroscopy applied to study of archaeological artefacts from Maligaimedu, Tamil Nadu, India, *Indian J. Pure Appl. Phys.*, vol. 45, no. 10, pp. 860–865, 2007
- <sup>45</sup> H. Rao, B. Li, Y. Yang, Q. Ma, and C. Wang, Proteomic identification of organic additives in the mortars of ancient Chinese wooden buildings, *Anal. Methods*, vol. 7, no. 1, pp. 143–149, 2015
- <sup>46</sup> S. Jayasingh and T. Selvaraj, Influence of organic additive on carbonation of air lime mortar—changes in mechanical and mineralogical characteristics, *Eur. J. Environ. Civ. Eng.*, vol. 0, no. 0, pp. 1–11, 2019
- <sup>47</sup> Ferreira, R. D. S., Anjos, M. A. S., Ledesma, E. F., Pereira, J. E. S., & Nóbrega, A. K. C. (2020). Evaluation of the physical-mechanical properties of cement-lime based masonry mortars produced with mixed recycled aggregates. *Materiales de Construcción*, 70(337), e210-e210
- <sup>48</sup> Anjos, M. A., Camões, A., Campos, P., Azeredo, G. A., & Ferreira, R. L. (2020). Effect of high-volume fly ash and metakaolin with and without hydrated lime on the properties of self-compacting concrete. *Journal of Building Engineering*, 27, 100985
- <sup>49</sup> Ferreira, R. L., Anjos, M. A., Nobrega, A. K., Pereira, J. E., & Ledesma, E. F. (2019). The role of powder content of the recycled aggregates of CDW in the behaviour of rendering mortars. *Construction and Building Materials*, 208, 601–612
- <sup>50</sup> K. A. Gour, R. Ramadoss, and T. Selvaraj, Revamping the traditional air lime mortar using the natural polymer – Areca nut for restoration application, *Constr. Build. Mater.*, vol. 164, pp. 255–264, 2018
- <sup>51</sup> C. Rodríguez-Navarro, Binders in historical buildings: Traditional lime in conservation, *Semin. SEM*, vol. 9, pp. 91–112, 2012
- <sup>52</sup> D. Miriello et al., Characterisation and provenance of lime plasters from the Templo Mayor of Tenochtitlan (Mexico city), *Archaeometry*, vol. 53, no. 6, pp. 1119–1141, 2011
- <sup>53</sup> C. Rispoli et al., Unveiling the secrets of Roman craftsmanship: mortars from Piscina Mirabilis (Campi Flegrei, Italy), *Archaeol. Anthropol. Sci.*, vol. 12, no. 1, 2020
- <sup>54</sup> S. Fernanda Carvalho, Methodologies for characterisation and repair of mortars of ancient buildings, *Hist. Constr. Int. Semin.*, pp. 353–362, 2001